

Mechanisms of Incipient Chemical Reaction between $\text{Ca}(\text{OH})_2$ and SiO_2 under Moderate Mechanical Stressing

III. Changes in the Short Range Ordering throughout the Mechanical and Thermal Processes

Tomoyuki Watanabe,¹ Tetsuhiko Isobe, and Mamoru Senna²

Faculty of Science and Technology, Keio University, 3-14-1 Hiyoshi, Yokohama 223, Japan

Received February 22, 1996; in revised form January 23, 1997; accepted February 6, 1997

The structure of mechanically induced precursor in an amorphous state between $\text{Ca}(\text{OH})_2$ and SiO_2 was determined by solid state MAS and CP/MAS ^{29}Si NMR spectroscopies, and the changes in the behavior of crystallization by linear heating were studied by X-ray diffractometry. A large broad Q_0 peak due to the short-range order of hydrated calcium silicates appeared in the ^{29}Si NMR spectra of mechanically induced precursors. The formation of the new ordering is confined in the near-surface region of SiO_2 particles, as confirmed by comparing MAS and CP/MAS NMR spectra. When the amorphous precursor obtained above was subsequently heated, a rapid solid state reaction led to single phased $\alpha\text{-CaSiO}_3$, as the final product.

© 1997 Academic Press

1. INTRODUCTION

In many cases, complex oxide precursors formed via a mechanochemical route are amorphous because of crystalline defects and/or being in a transition state of transformation (1). It is, therefore, difficult to determine the structure of such a precursor by X-ray diffractometry. Solid state high resolution nuclear magnetic resonance (NMR) spectroscopy is a versatile analytical tool to characterize a short-range order in such an amorphous precursor.

Ca–Si–O complex oxide system, treated in this paper, is closely related to those in cement chemistry. ^{29}Si solid state magic-angle-spinning (MAS) NMR has been used to study the local network structure of the C–S–H gel, where C denotes CaO; S, SiO_2 ; and H, H_2O , respectively, formed by the hydration of silicates (2–5).

The technique of cross polarization (CP)/MAS NMR is useful to observe resonances only from silicate species near

the hydroxyl groups of hydrated materials on the following basis. Magnetization is generated by excitation of ^1H nuclei, and then transfers to the ^{29}Si nuclei, so that the ^{29}Si species located in the vicinity of protons on a nanometer scale are preferentially observed by CP/MAS NMR spectroscopy (6–8).

The ^{29}Si MAS NMR spectra have been worked out in detail (5). They are resolved into five components, according to the contributions of the location of Si, i.e., those in isolated SiO_4 tetrahedra (Q_0), present at the end units of a chain (Q_1), in the middle units of chains (Q_2), at chain blanch sites (Q_3), and linked to four other SiO_4 tetrahedra (Q_4). The subscript N in Q_N indicates the coordination number of SiO_4 units around an Si atom. The ^{29}Si CP/MAS NMR spectroscopy detects the silanol groups on the surface of silica, e.g., Q_3 signal, assigned as SiO_4 units bound with three Si atoms and one OH group (7, 9). The difference in the chemical shifts of ^{29}Si NMR peaks between crystalline and amorphous states is generally not significant, although the peaks of the latter tend to be broader (10). The isotropic ^{29}Si chemical shift is closely related to molecular geometry, i.e., Si–O bond length (11, 12) and Si–O–Si bond angle (12, 13). The increase in the density of vitreous silica on heavy fast neutron irradiation is due, at least in part, to a reduction in the average Si–O–Si bond angle and, to a smaller extent, by a slight increase in the Si–O bond length (12). The changes in the distribution of these bonds due to mechanical activation are expected to be detected as well.

As we reported previously (14–16), Ca–O–Si bonding is formed in the course of incipient mechanochemical reaction between $\text{Ca}(\text{OH})_2$ and SiO_2 by two mechanisms, i.e., (I) an acid–base reaction between OH groups, one from $\text{Ca}(\text{OH})_2$ and the other from silanol groups, and (II) a radical recombination between O^- on $\text{Ca}(\text{OH})_2$ and E' center on SiO_2 at the interface of these dissimilar particles. In this paper, the short-range order of a mechanically induced precursor in an amorphous state is examined by solid state NMR spectroscopy. At the same time, changes to the final crystalline products with heating are studied by X-ray diffractometry

¹ Present address: Sankyo Co., Ltd., 1-2-58, Hiromachi, Shinagawaku, Tokyo 140, Japan.

² To whom all correspondence should be addressed. E-mail: senna@aplc.keio.ac.jp.

(XRD). Finally, we try to summarize the mechanisms from the incipient mechanochemical reaction to the thermal solid state processes between Ca(OH)₂ and SiO₂ as a consequence of mechanical treatment.

2. EXPERIMENTAL

A commercial reagent (Wako, Guaranteed grade, 99.9%) was used as a source of Ca(OH)₂. The specific surface area, S_B , was 7.2 m² g⁻¹, as determined by the BET method with N₂ adsorption. Fumed silica powder (Degussa, Aerosil 200, S_B 191 m² g⁻¹) was used as an SiO₂ source. As reported in our previous papers (14–16), 1 g of the mixture in the molar ratio Ca(OH)₂:SiO₂ = 3:4 was milled in air batchwise by a laboratory sized vibration mill (Glen-Creston). The amplitude, 50 mm, and the frequency, 12 Hz, were kept constant. Eight 9.8-mm nylon coated iron balls and a 26.1-cm³ cylindrical PTFE container were adapted. The milled mixtures are denoted CaS-*t*, where -*t* indicates the milling time in hours. An NMR spectrometer (Chemagnetics Inc., CMX-300) was used to determine the local structure around Si. MAS were acquired at a 4-kHz spinning rate with the samples placed in a Pyrex glass tube. The observation frequency was 59.6 MHz and the pulse decay was 10 s. The contact time was 2 ms. Polydimethylsilane was used as a secondary standard, of which the chemical shift was -34 ppm from tetramethylsilane (TMS). The assignment of an NMR peak is shown as Q_N . Differential thermal analysis (MAC Science-2020) was carried out by raising the temperature linearly at 10 K min⁻¹ in a stream of N₂ with a flow rate of 200 cm min⁻¹. The long-range ordering of the samples was observed by an X-ray diffractometer (Rigaku,

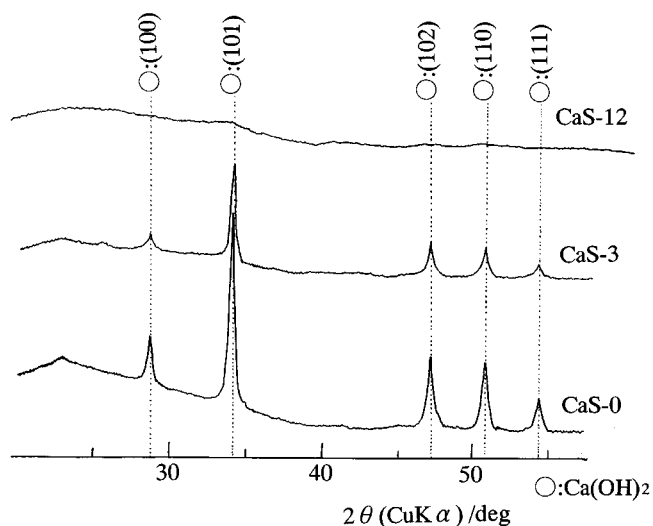


FIG. 1. XRD profiles of physically mixed Ca(OH)₂-SiO₂(CaS-0) and as-milled samples (CaS-3, CaS-12), where -*t* indicates milling time in hours. ○, Ca(OH)₂.

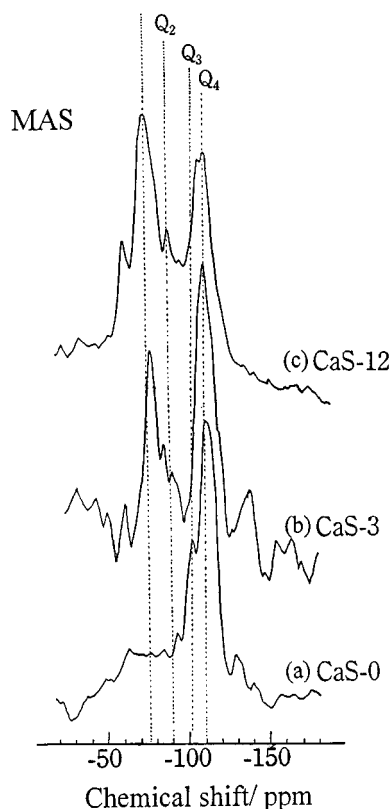


FIG. 2. ²⁹Si MAS NMR spectra of physically mixed(CaS-0) and milled samples(CaS-3,12), where -*t* indicates milling time in hours.

CN2013) using CuK α radiation. SiO₂ is expressed as S, CaSiO₃ as CS, Ca₂SiO₄ as C₂S, and Ca₃SiO₅ as C₃S.

3. RESULTS

3.1. Changes in the Si Coordination States Due to Mechanical Stress

The behavior of amorphization due to milling a mixture is shown in Fig. 1. The XRD peaks for Ca(OH)₂ disappear

TABLE 1
Assignments of Si NMR Chemical Shifts [2–11] (Chemical Shifts in ppm)

	Q_0	Q_1	Q_2	Q_3	Q_4
SiO ₂	nc ^a	nc	-91	-100.5	-100
Ca ₃ SiO ₅	-69–75	-79 ^b	-85 ^b	nc	nc
Ca ₂ SiO ₄	-71.4	nc	nc	nc	nc
β -CaSiO ₃	nc	nc	-89	nc	nc
α -CaSiO ₃	nc	nc	-83	nc	nc

^a Not observed or not identified.

^b These signals are likely to be attributed to the intermediate of the reaction to hydrated calcium silicates.

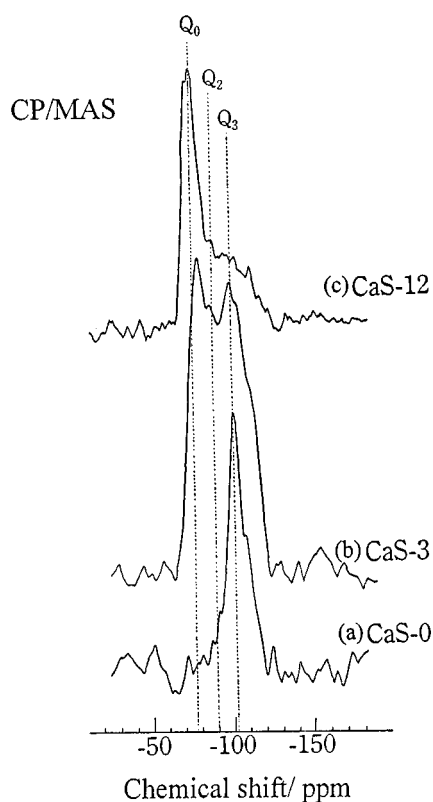


FIG. 3. ^{29}Si CP/MAS NMR spectra of physically mixed(CaS-0) and milled samples(CaS-3,12), where $-t$ indicates milling time in hours.

with milling for 12 h, being similar to the case of the $\text{Mg}(\text{OH})_2\text{-SiO}_2$ system (17). The changes in the Si coordination state due to mechanical stress is visualized by the

chemical shift of ^{29}Si MAS and CP/MAS NMR spectrograms, shown in Figs. 2 and 3, respectively. The assignment of respective chemical shifts according to Refs. (2–11) is given in Table 1. Since two kinds of Si, bound to surface silanol groups and linked to four other SiO_4 tetrahedra, are observed for pure Aerosil silica (9), the peaks at -100 and -110 ppm in Fig. 2a are assigned as Q_3 and Q_4 , respectively.

When a mixture is milled, a large broad Q_0 peak at -75 ppm is observed in Figs. 2b and 2c. The Q_0 peak is accompanied by shoulders of Q_2 at -89 ppm. The peaks derived from original silica, Q_3 and Q_4 , are still observed after milling for 12 h. The signals Q_0 and Q_2 are likely to be attributed either to the intermediate of the reaction to calcium silicates with and without hydration. A peak at around -60 ppm on CaS-12 (Fig. 2c) cannot be assigned at the moment.

In the ^{29}Si CP/MAS NMR spectrum, giving information preferentially for ^{29}Si near a surface silanolic proton, the Q_3 peak for silanol groups of pure silica is predominant in a mixture without milling, as shown in Fig. 3a. The Q_4 peak was hardly observed. This implies that most of the silicon atoms near the surface of SiO_2 particles link to silanolic OH groups. When a mixture is milled for 3 h, however, the Q_3 peak overlaps with Q_0 . After 12 h, the Q_0 peak grows to be predominant, while Q_3 almost disappears. It is to be noted that the Q_0 peak in both MAS and CP/MAS NMR increase with milling with a preferential decrease in the Q_3 peak, while Q_4 is observed only by MAS NMR. From these observations, it seems safe to assume that the short-range ordering corresponding to calcium silicates is formed near a proton, since Q_0 is mainly attributed to hydrated calcium silicates.

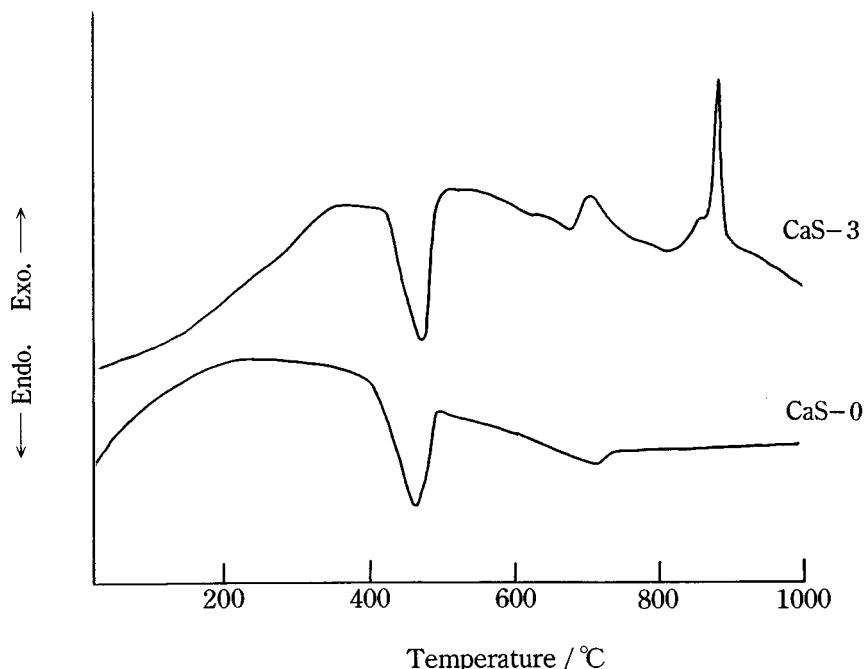


FIG. 4. DTA profiles of physically mixed (CaS-0) and milled (CaS-3) samples.

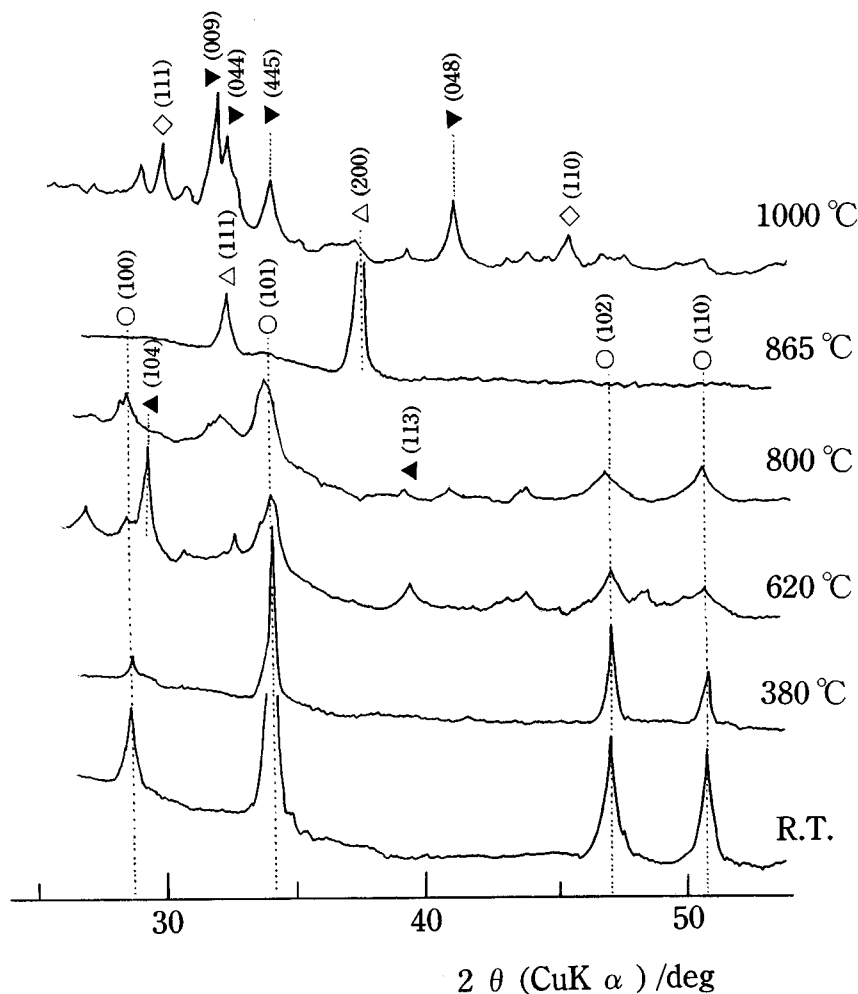


FIG. 5. XRD profiles of CaS-0 heated at 10 K min^{-1} up to temperatures ($^{\circ}\text{C}$) indicated in the right margin. \circ , $\text{Ca}(\text{OH})_2$; \blacktriangle , CaCO_3 ; \triangle , CaO ; \blacktriangledown , Ca_3SiO_5 ; \diamond , SiO_2 .

3.2. Changes in the Thermal Behavior with Mechanical Activation

As shown in Fig. 4, a new exothermic peak is observed around 880°C in the DTA profile of the mixture milled for 3 h, CaS-3, while no exothermic peak was detected in the physically mixed sample CaS-0. XRD analysis was, therefore, carried out for the samples CaS-0 and CaS-3 to examine the consequences of mechanical treatment during subsequent heating.

The remarkable difference in the XRD profiles between the two samples are appreciable above 800°C , as shown in Figs. 5 and 6 for CaS-0 and CaS-3, respectively. After heating up to 865°C , only the XRD peaks of CaO are observed in the XRD profile of the sample CaS-0, while a halo pattern is observed for CaS-3. At 1000°C , only the XRD peaks of $\alpha\text{-CaSiO}_3$ (pseudowollastonite) are observed on the mixture with preliminary milling. In contrast, the

peaks of Ca_3SiO_5 and unreacted SiO_2 are detected in the XRD profiles of the physically mixed sample. The exothermic DTA peak at 880°C in Fig. 4 for the sample CaS-3 is, therefore, likely to be caused by the crystallization of $\alpha\text{-CaSiO}_3$.

4. DISCUSSION

4.1. Mechanisms of Incipient Mechanochemical Reaction

From the comparison between MAS and CP/MAS signals stated at the end of Section 3.1, we conclude that the complex oxide precursor having a short-range structure of hydrated calcium silicates is formed only near the surface region of the SiO_2 particles with surface silanol groups. This is compatible with our previous observation, where the reduction of Si^{4+} to Si^{2+} due to electron transfer to Si^{4+} through a Ca-O-Si bond is restricted to the region of a single nanometer, as confirmed by X-ray photoelectron

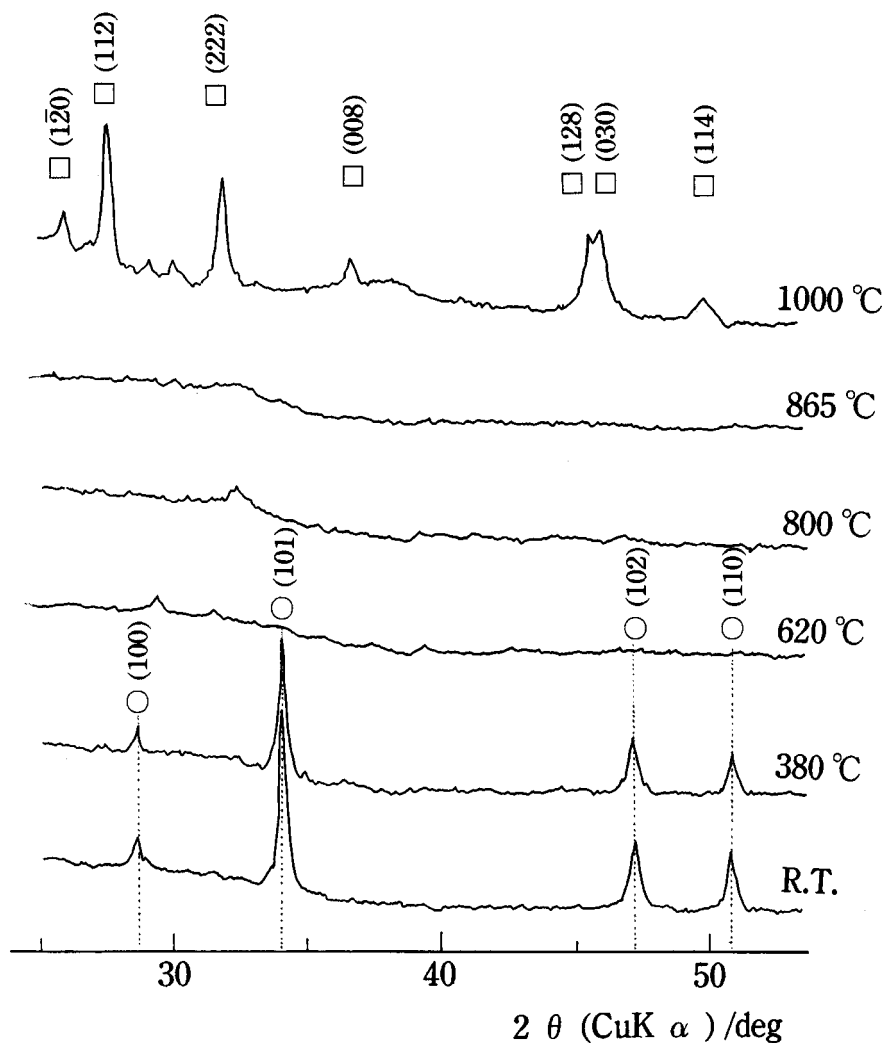


FIG. 6. XRD profiles of CaS-3 heated at 10 K min^{-1} up to temperatures ($^{\circ}\text{C}$) indicated in the right margin. \circ , Ca(OH)_2 ; \square , $\alpha\text{-CaSiO}_3$.

spectroscopy in the $\text{Ca(OH)}_2\text{-SiO}_2$ system (15) coupled with an Ar^+ etching.

A nonmilled mixture has abundant silanol groups, while silicon atoms keep a tetravalent electronic state, as confirmed by previous XPS studies (15). The reduction of Si^{4+} to Si^{2+} is accomplished by the formation of Ca–O–Si bonds through an acid–base reaction as well as a radical recombination during milling. The reduction of Si^{4+} never occurs when SiO_2 is milled alone even for a long time. Therefore, the reduction of Si^{4+} to Si^{2+} is a consequence of the electron transfer from calcium to silicon via Ca–O–Si bonding toward higher electronegativity of Si. This electron transfer can be explained by Sanderson's theory (19), who proposed a general principle of balance of electron density between two atoms with different electronegativities. The principle can also be applied in the present case, where the changes in the coordination number due to locally and

irreversibly deformed crystals are involved. As a result of the increase in the electron density of Si due to such a reduction, the electronic repulsion between localized core electrons in Si^{2+} and O^{2-} increases. This results in the elongation, and hence, weakening of the Si–O bonds. This, in turn, leads to easier breakage of these bonds during mechanical stressing.

In this mechanochemical process toward calcium silicate formation, the diffusion species are likely to be both Ca^{2+} and O^{2-} of CaO, as known in conventional glass chemistry (20), since the Ca–O bond energy is weaker than that of Si–O. From the result of milling a mixture for 12 h, turning to noncrystalline in XRD analysis (Fig. 1), almost all Ca(OH)_2 seems to have reacted with SiO_2 . However, unreacted SiO_2 is detected by MAS NMR spectroscopy as shown in Fig. 2c. A hydrated calcium silicate precursor having a Ca-rich composition is observed by both MAS and

CP/MAS NMR spectroscopies as shown in Figs. 2 and 3, respectively. In a conventional thermal reaction, the diffusion rate of Ca²⁺ is known to be higher than that of Si⁴⁺ (20). This seems also to be the case in the present mechanochemical process. Thus, Ca²⁺ and O²⁻ from CaO, formed by mechanochemical dehydration of Ca(OH)₂, migrate into the SiO₂ matrix across the interface. One tetrahedral SiO₄ unit has three weakened Si–O bonds and the fourth as Si–O–Ca on the surface. Thus, more than two Ca²⁺ ions from CaO, generated by mechanochemical dehydration of Ca(OH)₂, can be coordinated for one SiO₄ unit.

4.2. Mechanisms of Thermal Reactions for Mechanically Activated Samples

The mechanisms of solid state reactions in this system are discussed on the basis of NMR and XRD analyses. Mechanical stressing on the Ca(OH)₂ and SiO₂ particles produces various surface defects, e.g., the lower coordination number on the surface as confirmed by ¹H NMR and IR (15) and the cation and anion point defects by EPR (16). The thermal diffusion of Ca²⁺ and O²⁻ at the Ca(OH)₂–SiO₂ interface at elevated temperature is enhanced through these defects in the mechanically activated samples. Thus, crystalline CaO formed in a physical mixture with heating, as shown in Fig. 5, does not survive in a milled mixture, as shown in Fig. 6, since the solid solution in the amorphous state is already formed at 865°C. As mentioned in Section 3.1, a Ca-rich complex oxide precursor exists on the surface of SiO₂ when a mixture is milled. The concentration gradient of Ca²⁺, being an important driving force of thermal diffusion, is larger between the calcium-rich silicate precursor phase and unreacted SiO₂ than that between the precursor and unreacted Ca(OH)₂. This is demonstrated by Fig. 6, where solid state reaction progresses toward reducing the Ca/Si ratio leading to formation of a single phase of α-CaSiO₃.

5. CONCLUSION

Mechanochemical reaction between Ca(OH)₂ and SiO₂ produces an amorphous precursor, with the short-range order of hydrated calcium silicates in the vicinity of a proton near the surface of SiO₂ particles. Formation of a single

phased α-CaSiO₃ occurs when a mixture is heated after milling. The proposed mechanism based on the formation of short-range ordering of complex oxides could widely be applied to other complex oxide systems as well, as far as the incipient solid state acid–base reaction under mechanical stressing is possible.

ACKNOWLEDGMENT

The authors thank Mr. Sugisawa at JEOL Ltd. for NMR measurements.

REFERENCES

1. M. Senna, *J. Solid State Ionics* **63–65**, 3 (1993).
2. M. Magi, E. Lippmaa, A. Samoson, G. Engelhardt, and A. R. Grimmer, *J. Phys. Chem.* **88**, 1518 (1984).
3. G. W. Groves, A. Brough, I. G. Richardson, and C. M. Dobson, *J. Am. Ceram. Soc.* **74**, 2891 (1991).
4. H. Ishida, K. Sasaki, Y. Okada, and T. Mitsuda, *J. Am. Ceram. Soc.* **75**, 2541 (1992).
5. A. R. Brough and C. M. Dobson, *J. Am. Ceram. Soc.* **77**, 593 (1994).
6. A. Comotti, G. Castaldi, C. Gilioli, G. Torri, and P. Sozzani, *J. Mater. Sci.* **29**, 6427 (1994).
7. S. Leonardelli, L. Facchini, C. Fretigny, P. Tougne, and A. P. Legrand, *J. Am. Chem. Soc.* **114**, 6412 (1992).
8. A. R. Brough, C. M. Dobson, I. G. Richardson, and G. W. Groves, *J. Mater. Sci.* **29**, 3926 (1994).
9. V. V. Brei, *J. Chem. Soc. Faraday Trans.* **90**, 2961 (1994).
10. S. Hayashi, K. Okada, and N. Otsuka, *J. Eur. Ceram. Soc.* **14**, 61 (1994).
11. J. Skibsted, J. Hjorth, and H. Jackobsen, *Chem. Phys. Lett.* **172**, 279 (1990).
12. A. C. Wright, B. Bachra, T. M. Brunier, R. N. Sinclair, L. F. Gladden, and R. L. Portsmouth, *J. Non-Cryst. Solids* **150**, 69 (1992).
13. R. F. Pettifer, R. Dupree, I. Farman, and U. Sternberg, *J. Non-Cryst. Solids* **106**, 408 (1988).
14. T. Watanabe, J. Liao, and M. Senna, *J. Solid State Chem.* **115**, 390 (1995).
15. T. Watanabe, T. Isobe, and M. Senna, *J. Solid State Chem.* **122**, 74 (1996).
16. T. Watanabe, T. Isobe, and M. Senna, *J. Solid State Chem.* **122**, 291 (1996).
17. J. Liao and M. Senna, *J. Solid State Ionics* **66**, 313 (1993).
18. T. Okada, H. Shibasaki, and T. Masuda, *Onoda kenkyuhoukoku* **45**, 126 (1994).
19. R. T. Sanderson, *Science* **114**, 670 (1951).
20. W. D. Kingery, H. K. Bowen, and D. R. Uhlmann, "Introduction to Ceramics," p. 262. Wiley, New York, 1976.